Transactions D:
Computer Science & Engineering and
Electrical Engineering
Vol. 17, No. 2, pp. 163–174

SCIENTIA IRANICA

Simultaneous Coordinated Tuning of SSSC-Based Stabilizer and PSS Using Quadratic Mathematical Programming

M.R. Shakarami[1,*] and A. Kazemi[1]

Abstract. *In a Static Synchronous Series Compensator (SSSC), a controllable AC voltage is generated by a voltage-source converter. There are two control channels for controlling the magnitude and phase of the voltage. When this device is used for damping inter-area oscillations in multi-machine power systems, a damping stabilizer can be included in both channels. In this paper, a method for the simultaneous coordinated design of a Power System Stabilizer (PSS) and a SSSC-based stabilizer is presented using quadratic mathematical programming. In this method, the gain and phase of a lead-lag stabilizer can be simultaneously calculated. By this method the effect of the SSSC-based stabilizer in both control channels on damping inter-area oscillations has been assessed. Obtained results including eigenvalue analysis and non-linear simulations, on two multi-machine power systems under different operating conditions, show that the usage of a SSSC stabilizer in a suitable control channel can significantly reduce the control cost of the stabilizer.*

Keywords: *Damping stabilizer; Inter-area oscillations; SSSC; PSS; Quadratic mathematic programming.*

INTRODUCTION

The damping of power system oscillations between inter-connected areas is very important for secure operation of the system [1]. Conventionally, Power System Stabilizers (PSSs) are used for damping power system oscillations. The damping of inter-area oscillations may be reduced significantly in stressed power systems [2]. In this case, the use of PSSs may not only be effective in providing sufficient damping for inter-area oscillations [3]. While PSSs have the capability to damp local modes, series power electronics-based FACTS stabilizers have become amongst the best alternative means to improve damping inter-area oscillations. However, interactions between PSSs and FACTS-based stabilizers may enhance or degrade the damping of certain oscillation modes. Therefore, coordinated parameter design of PSSs and FACTS stabilizers is necessary to improve overall system performance. SSSC is one of the series FACTS devices that in addition to increasing transferred power can improve the stability of power systems [4-7]. The SSSC, in comparison with other FACTS devices, is more effective for damping mechanical oscillations [8]. The SSSC injects a set of balanced voltages to the transmission line quadrature with the line current. There are two control channels to control the magnitude and phase of the voltage, which are magnitude control and phase control channels. When the SSSC is used for damping mechanical oscillations, the damping stabilizer can be included in both channels. Most studies are done on SSSC magnitude-based stabilizers [9-13]. It seems that the SSSC phase-based stabilizer is not basically studied in reported literature. Therefore, the effect of a SSSC-based stabilizer in different control channels on damping inter-area oscillations in multi-machine power systems needs to be evaluated.

One effective method in designing damping stabilizers in FACTS devices is linear programming [14,15]. However, in these papers, the first phase of a stabilizer has been calculated and, assuming that the stabilizer

1. *Department of Electrical Engineering, Iran University of Science and Technology, Tehran, P.O. Box 16846, Iran.*
*. *Corresponding author. E-mail: shakarami@iust.ac.ir*

Received 9 September 2009; received in revised form 29 December 2009; accepted 16 February 2010

phase remains constant in the frequency range of oscillation modes, using linear programming the gain of the stabilizer has been calculated. This assumption may not be true [16]. In [17], the gain and phase of a PSS have simultaneously been calculated using mathematic programming. In this paper, it is supposed that the phase of the residue is positive therefore, PSS must have a lead phase structure. However, in some cases particularly in FACTS-based stabilizers the phase of the residue can be negative and the stabilizer must have a lag structure.

In this paper, a SSSC-based stabilizer is investigated in order to improve damping inter-area oscillations in multi-machine power systems. In addition to a magnitude-based stabilizer, a phase-based stabilizer is presented for SSSC. A method based on quadratic mathematic programming to design a phase-lead or a phase-lag damping stabilizer has been presented. This method is used for simultaneous parameter design of a SSSC-based stabilizer and a PSS to improve the dynamic stability of power systems. By this method, the effect of different stabilizers of SSSC on damping inter-area oscillations in two machine power systems under different operating conditions has been analyzed and compared.

POWER SYSTEM MODEL

Generator

In this study, the generators are represented by a forth-order $d-q$ axis model. In this case, nonlinear dynamic equations for each generator with known variables are [18]:

$$\dot{\delta} = \omega - \omega_s, \tag{1}$$

$$M\dot{\omega} = P_m - P_e - D\left(\frac{\omega}{\omega_s} - 1\right), \tag{2}$$

$$T'_{d0}\dot{E}'_q = -E'_q - (X_d - X'_d)I_d + E_{FD}, \tag{3}$$

$$T'_{q0}\dot{E}'_d = -E'_d + (X_q - X'_q)I_q, \tag{4}$$

$$P_e = (I_d E'_d + I_q E'_q) + (X'_q - X'_d)I_d I_q, \tag{5}$$

where δ, ω, ω_s, M, D and P_m are angle, speed, synchronous speed, inertia, damping coefficient and input mechanical power of the machine, respectively; x_d, x_q, i_d, i_q, x'_d and x'_q are d-axis reactance, q-axis reactance, d-axis current, q-axis current, d-axis transient reactance and q-axis transient reactance, respectively; T'_{do} and T'_{qo} are q- and d open circuit time constant, respectively; E_{FD} is the filed voltage, and E'_q and E'_d are the quadrature and direct axis component of transient voltage, respectively.

Exciter

The IEEE type-AC-4A excitation system is considered in this work. Its block diagram is shown in Figure 1. The role of used parameters for the system is discussed in [19]. For stability improvement, the exciter of each generator can be equipped with a PSS, as shown in Figure 1, where V_T and V_{REF} are the terminal voltage of the generator and reference of voltage regulator, respectively. K_A is gain and T_R, T_A, T_B and T_C are time constants related to the excitation system.

SSSC Modeling

It is assumed that in a multi-machine power system a SSSC is installed on the transmission line between nodes 1 and 2, as shown in Figure 2.

The SSSC consists of a Series Coupling Transformer (SCT) with the leakage reactance, X_{SCT}, a three-phase GTO based Voltage Source Converter (VSC) and a DC capacitor. The SSSC can be described as [9]:

$$V_{inj} = mkV_{dc}(\cos\phi + j\sin\phi), \tag{6}$$

$$I_L = I_D + jI_Q = |I_L|\angle\psi, \tag{7}$$

$$\frac{dV_{dc}}{dt} = \frac{mk}{C_{dc}}(I_D\cos\phi + I_Q\sin\phi), \tag{8}$$

where V_{inj} is the ac injected voltage by the SSSC; m and ϕ are the modulation ratio and phase defined by

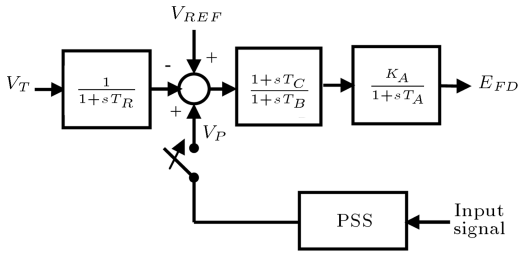

Figure 1. Excitation system.

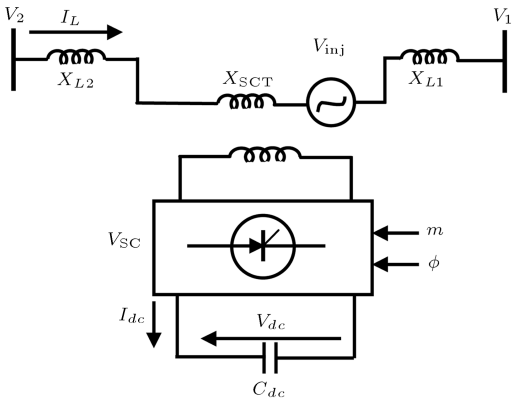

Figure 2. SSSC structure.

Pulse Width Modulation (PWM), respectively; k is the ratio between the ac and dc voltage depending on the converter structure; V_{dc} is the dc voltage; C_{dc} is the dc capacitor value, and I_D and I_Q are D-and Q components of the line current I_L, respectively.

SSSC-BASED STABILIZERS

Phase-Based Stabilizer

Assuming a lossless SSSC, the ac voltage is kept in quadrature with the line current so that the SSSC only exchanges reactive power with the transmission line. By adjusting the magnitude of the injected voltage, the reactive power exchange can be controlled. When the SSSC voltage lags the line current by 90°, it emulates a series capacitor. It can also emulate a series inductor when the voltage leads the line current by 90°. Thus, a SSSC can be considered as a series reactive compensator where the degree of compensation can be varied by controlling the magnitude of the injected voltage. In this paper, the SSSC is considered in capacitor mode. To keep the injected voltage in quadrature with the line current, a PI controller, as shown in Figure 3, has been used. Here, ϕ_{ref} is the phase of the injected voltage in steady-state and its value is considered $\phi_{\text{ref}} = -90° + \psi_{ss}$ where ψ_{ss} is the angle of the line current in steady-state; T_s is time constant of the converter, and K_P and K_I are the proportional and integral gain of the PI controller, respectively. A lead-lag stabilizer for damping inter-area oscillations is included in the PI controller. In this case the stabilizer is called the phase-based stabilizer and, for convenience in this paper, it is called the ϕ-based stabilizer. In this stabilizer, T_W is washout time constant usually in the range of 1 to 15 s. To design the stabilizer, usually the value of T is assumed as pre-specified, and x_2, x_1 and x_0 are parameters to be determined. In this paper, the adopted value of T for the stabilizer is considered according to the typical values in the studied literature, especially the typical value for PSS presented in [18,19].

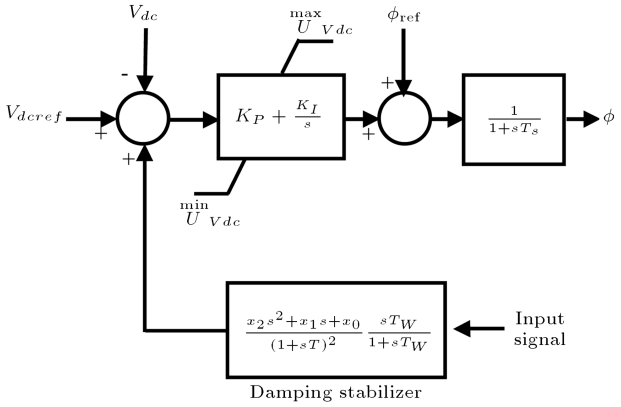

Figure 3. SSSC phase controller with a damping stabilizer.

The feedback signal for the stabilizer is selected among local signals such as the line-current, the line-real power and the line-reactive power.

Magnitude-Based Stabilizer

To control the magnitude of the injected voltage, modulation ratio m can be controlled. Figure 4 shows the block diagram of the controller in this case where m_{ref} is the value of modulation ratio in steady state. A stabilizer for the damping of inter-area oscillations is included in the magnitude controller. This stabilizer is called the m-based stabilizer.

STABILIZER DESIGN

The method adopted in this work to design a SSSC stabilizer is an incremental method. This method is summarized as follows. In the first step, the closed-loop system is considered, as in Figure 5, where $G(s)$ and $\overline{F}(s)$ are the power system transfer matrix and the stabilizer transfer matrix, respectively. In the second step, the stabilizer transfer matrix is changed by ΔF. In this case, the closed-loop system changes, as shown in Figure 6, where $\overline{G}(s)$ is the transfer matrix of the inner loop between $G(s)$ and $\overline{F}(s)$. In these figures, U_{ref} is considered as the input signal of the system. In the SSSC-based stabilizer in the phase control channel, U_{ref} is replaced by V_{dcref}, and in the magnitude control channel, it is replaced by m_{ref}. For a PSS, U_{ref} is replaced by V_{REF}. One of the local signals is selected

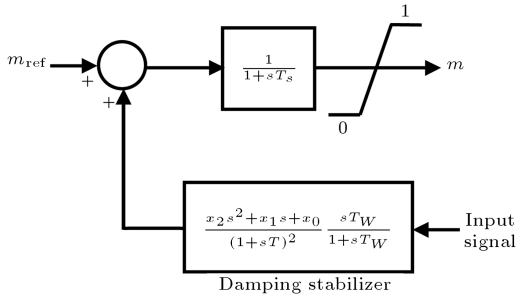

Figure 4. SSSC magnitude controller with a damping stabilizer.

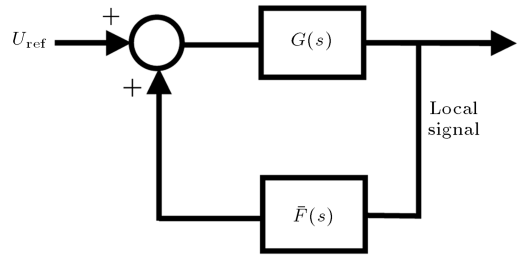

Figure 5. Closed-loop system in the first step.

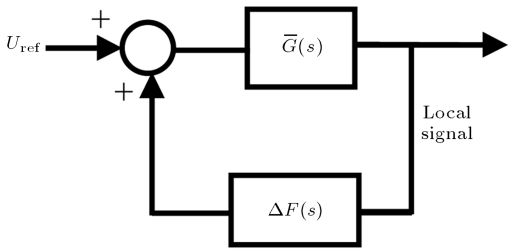

Figure 6. Closed-loop system in the second step.

as the feedback signal for SSSC-based stabilizers. For a PSS, the generator acceleration power is chosen as the feedback signal. The value of ΔF is calculated to shift eigenvalues of critical modes to desired values.

In the following, a procedure for the calculation of ΔF is presented. Assuming that the variation of ΔF is sufficiently small, the variation of the eigenvalue, λ_i, can be approximated as:

$$\Delta\lambda_i = \sum_{q=1}^{n_s} \rho_{iq} \Delta f_q(\lambda_i), \qquad (i = 1, 2, \cdots, n), \tag{9}$$

where n is the number of critical eigenvalues; n_s is the number of stabilizers and ρ_{iq} is the residue associated to the ith eigenvalue λ_i of $\overline{G}(s)$ for the qth stabilizer. Equation 9 can be rewritten as:

$$\begin{aligned}\Delta\lambda_i = &\sum_{q=1}^{n_s} \{\mathrm{Re}(\rho_{iq})\mathrm{Re}(\Delta f_q(\lambda_i)) \\ &- \mathrm{Im}(\rho_{iq})\mathrm{Im}(\Delta f_q(\lambda_i))\} \\ &+ j \sum_{q=1}^{n_s} \{\mathrm{Re}(\rho_{iq})\mathrm{Im}(\Delta f_q(\lambda_i)) \\ &+ \mathrm{Im}(\rho_{iq})\mathrm{Re}(\Delta f_q(\lambda_i))\}. \end{aligned} \tag{10}$$

It is assumed that the qth stabilizer has a lead-lag structure as follows:

$$f_q(s) = \frac{x_{q_2} s^2 + x_{q_1} s + x_{q_0}}{(1 + sT_q)^2} \frac{sT_w}{1 + sT_w}. \tag{11}$$

By substituting $s = \lambda_i$ and $x_{qz} = \Delta x_{qz} (z = 1, 2, 3)$ in Equation 11, the real and imaginary part variations of $\Delta f_q(\lambda_i)$ are:

$$\mathrm{Re}(\Delta f_q(\lambda_i)) = R_{2qi}\Delta x_{q2} + R_{1qi}\Delta x_{q1} + R_{0qi}\Delta x_{q0}, \tag{12}$$

$$\mathrm{Im}(\Delta f_q(\lambda_i)) = I_{2qi}\Delta x_{q2} + I_{1qi}\Delta x_{q1} + I_{oqi}\Delta x_{q0}, \tag{13}$$

where R_{0qi}, R_{1qi}, R_{2qi}, I_{0qi}, I_{1qi}, and I_{2qi} are specified values. To shift critical eigenvalues to the left of the imaginary axis, we must have:

$$\mathrm{Re}(\Delta\lambda_i) \leq -|\Delta\sigma_i|, \tag{14}$$

$$-|\Delta\omega_i| \leq \mathrm{Im}(\Delta\lambda_i) \leq |\Delta\omega_i|, \tag{15}$$

where $\Delta\sigma_i$ and $\Delta\omega_i$ are the desired shift value of the real part and acceptable frequency variations of the critical eigenvalue, λ_i, respectively. Substituting Equations 12 and 13 in Equation 10, we can obtain $\Delta\lambda_i$ as a linear function from Δx_{q_2}, Δx_{q_1} and Δx_{q_0}. Substituting the real part of $\Delta\lambda_i$ in Equation 14 and its imaginary part in Equation 15 then yields:

$$\sum_{q=1}^{n_s} \{\alpha_{2qi}\Delta x_{q2} + \alpha_{1qi}\Delta x_{q1} + \alpha_{0qi}\Delta x_{q0}\} \leq -|\Delta\sigma_i|, \tag{16}$$

$$\begin{aligned} -|\Delta\omega_i| &\leq \sum_{q=1}^{n_s} \{\beta_{2qi}\Delta x_{q2} + \beta_{1qi}\Delta x_{q1} + \beta_{0qi}\Delta x_{q0}\} \\ &\leq |\Delta\omega_i|, \end{aligned} \tag{17}$$

where α_{0qi}, α_{1qi}, α_{2qi}, β_{0qi}, β_{1qi} and β_{2qi} are specified values. On the other hand, if the angle of residue, ρ_{qi}, is positive, the qth stabilizer must have a phase-lead characteristic, otherwise it must have a phase-lag characteristic.

Considering $\bar{s} = sT_q$, $\widehat{x}_{q2} = x_{q2}/(x_{qo}T_q^2)$ and $\widehat{x}_{q1} = x_{q1}/(x_{q0}T_q)$, and substituting them in Equation 11 yields:

$$f_q(\bar{s}) = x_{q0} \frac{\widehat{x}_{q2}\bar{s}^2 + \widehat{x}_{q1}\bar{s} + 1}{(1 + \bar{s})^2} \frac{T_w\bar{s}}{T_q + T_w\bar{s}}. \tag{18}$$

According to [20] for a phase-lead structure, it is assumed that zeroes of $\overline{f}_q(s)$ are almost one-decade nearer to the center than that of its poles, i.e. they belong to interval $[-1 \ -0.1]$, and for the phase-lag structure, the zeroes are almost one-decade farther to the center, i.e. they belong to interval $[-10 \ -1]$. This subject is graphically shown for lead and lag structures in Figures 7 and 8, respectively. In these figures, the points inside the triangles and above the parabolas correspond to the above intervals. To represent the constraints as a linear function, the parabolas are approximated by lines. In this case, the zeroes may be complex values, but the real parts of the complex zeroes are located in the above intervals.

According to Figure 7, the constraints for a phase lead structure can be written as:

$$\widehat{x}_{q1} - \widehat{x}_{q2} \leq 1, \tag{19}$$

$$\widehat{x}_{q1} - 0.1\widehat{x}_{q2} \leq 10, \tag{20}$$

$$-99x_{q1} + 18x_{q2} \leq -180. \tag{21}$$

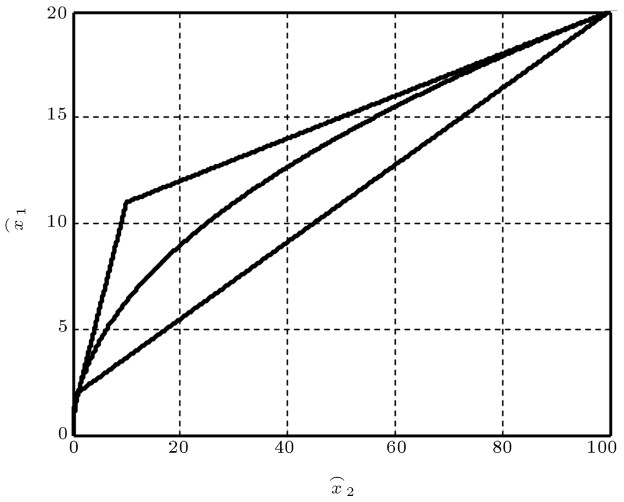

Figure 7. Region corresponding to phase-lead stabilizer.

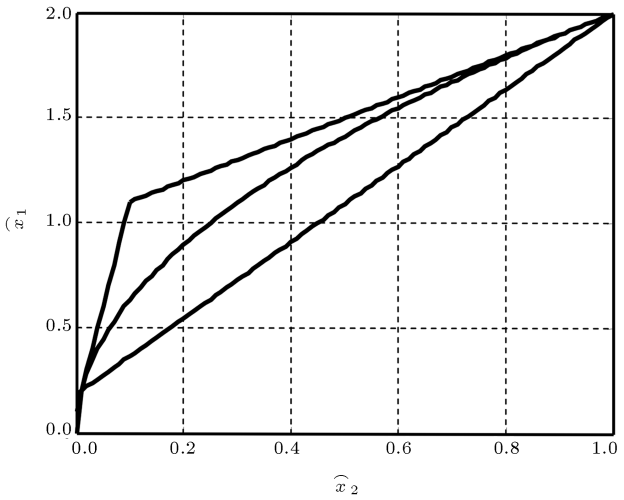

Figure 8. Region corresponding to phase-lag stabilizer.

As illustrated in Figure 8, the constraints for the phase lag stabilizer are:

$$\widehat{x}_{q1} - \widehat{x}_{q2} \leq 1, \tag{22}$$

$$10\widehat{x}_{q1} - 100\widehat{x}_{q2} \leq 1, \tag{23}$$

$$-99\widehat{x}_{q1} + 180\widehat{x}_{q2} \leq -18. \tag{24}$$

Substituting $\widehat{x}_{q2}$ and $\widehat{x}_{q1}$ in Equations 19 to 24, and assuming $x_{qz} = \Delta x_{qz} + \bar{x}_{qz}(z = 1,2,3)$ where $\bar{x}_{q0}$, $\bar{x}_{q1}$ and $\bar{x}_{q2}$ are known values, the constraints can be rewritten for the lead structure as Equations 25 to 27, and for the lag structure as Equations 28 to 30:

$$-\Delta x_{q2} + T_q \Delta x_{q1} - T_q^2 \Delta x_{q0} \leq \bar{x}_{q2} - T_q \bar{x}_{q1} + T_q^2 \bar{x}_{q0}, \tag{25}$$

$$-\Delta x_{q2} + 10T_q \Delta x_{q1} - 100T_q^2 \Delta x_{q0} \leq \bar{x}_{q2} - 10T_q \bar{x}_{q1} + 100T_q^2 \bar{x}_{q0}, \tag{26}$$

$$18\Delta x_{q2} - 99T_q \Delta x_{q1} + 180T_q^2 \Delta x_{q0} \leq -18\bar{x}_{q2} + 99T_q \bar{x}_{q1} - 180T_q^2 \bar{x}_{q0}, \tag{27}$$

$$-\Delta x_{q2} + T_q \Delta x_{q1} - T_q^2 \Delta x_{q0} \leq \bar{x}_{q2} - T_q \bar{x}_{q1} + T_q^2 \bar{x}_{q0}, \tag{28}$$

$$-100\Delta x_{q2} + 10T_q \Delta x_{q1} - T_q^2 \Delta x_{q0} \leq 100\bar{x}_{q2} - 10T_q \bar{x}_{q1} + T_q^2 \bar{x}_{q0}, \tag{29}$$

$$180\Delta x_{q2} - 99T_q \Delta x_{q1} + 18T_q^2 \Delta x_{q0} \leq -180\bar{x}_{q2} + 99T_q \bar{x}_{q1} - 18T_q^2 \bar{x}_{q0}. \tag{30}$$

The following function, as the gain of the stabilizer at the frequency $\bar{\omega}_p$, $p = 1, 2, \cdots, N$, is considered to be the objective function [17]:

$$J = \min \sum_{p=1}^{N} \sum_{q=1}^{n_s} \left| f_q(j\bar{\omega}_p) \right|^2, \tag{31}$$

where $\bar{\omega}_1, \bar{\omega}_2, \cdots, \bar{\omega}_N$ are a set of frequencies in the region where the critical eigenvalue must be shifted.

By substituting Equation 11 in Equation 31 and considering $s = j\bar{\omega}_p$ and $X = \bar{X} + \Delta X$, we can easily rewrite the objective function as:

$$J = \min \frac{1}{2} \Delta X^T H \Delta X + f^T \Delta X, \tag{32}$$

where the matrix H, vector f and vector $\bar{X}$ are known, and ΔX is the unknown vector to be tuned where:

$$\bar{X} = \begin{bmatrix} \bar{x}_{n_s 2} & \bar{x}_{n_s 1} & \bar{x}_{n_s 0} & \cdots & \bar{x}_{12} & \bar{x}_{11} & \bar{x}_{10} \end{bmatrix}^T,$$

$$\Delta X = \begin{bmatrix} \Delta x_{n_s 2} & \Delta x_{n_s 1} & \Delta x_{n_s 0} & \cdots & \Delta x_{12} & \Delta x_{11} & \Delta x_{10} \end{bmatrix}^T.$$

Equation 32 with Equations 16 to 17, and Equations 25 to 27 or Equations 28 to 30 is as a quadratic mathematical programming problem. To solve this problem, the quadprog algorithm provided by the Matlab Optimization Toolbox is applied here. The proposed approach is an iterative method. In this method, the calculated vector of ΔX is added to the known vector, $\bar{X}$, and it is considered as a known vector in the next iteration. The vector, $\bar{X}$, in the first iteration is set to be zero.

SIMULATION RESULTS

Two-Area Four-Machine Power System

A single line diagram of the system is shown in Figure 9. Data of this system are represented in [21]. The loads are modeled as constant impedances. To increase transferred power, the load in area 2 has been increased and the load in area 1 has then been modified to achieve a given tie-line transferred power.

A local signal with maximum residue for inter-area mode is selected as a feedback signal for the damping stabilizer. Figure 10 shows the magnitude of residues as a function of transmitted power for different local signals. It can be concluded from this figure that:

i) When the stabilizer is included in the phase control channel (the ϕ-based stabilizer), the residues for the inter-area mode for different local feedback signals are higher than those for cases when the stabilizer is included in the magnitude control channel (the m-based stabilizer).

ii) Variation of the current in the transmission line, where the SSSC is installed, is the best signal for both stabilizers.

Typically, operation conditions presented in Table 1 are considered. The parameters of the PI controller are calculated as follows.

To obtain a suitable response for the system at a certain operation condition, for a positive value of

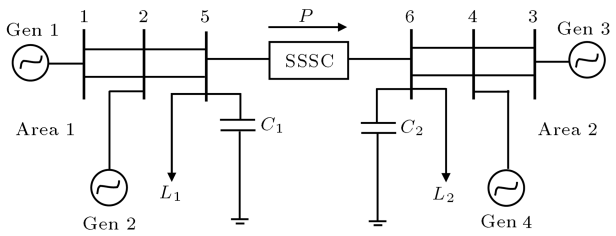

Figure 9. One-line diagram of the 4-machine power system.

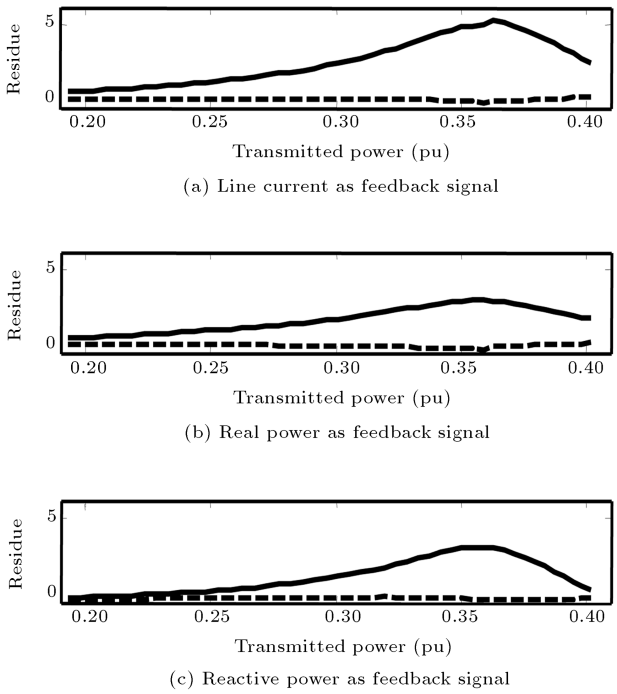

Figure 10. Magnitude of residue for inter-area mode. Solid line: SSSC phase-based stabilizer; dashed line: SSSC magnitude-based stabilizer.

K_I, the value of K_P is increased so that the modes related to the phase-controller (controller modes) are stable. Also, the PI controller must not have significant degraded effects on damping mechanical oscillations. Then, the values that are suitable for all considered operation conditions are selected. For operation conditions presented in Table 1, K_P and K_I are approximately calculated as $200 \leq K_I \leq 450$ and $25 \leq K_P \leq 120$.

Considering $K_P = 25$ and $K_I = 200$, the open-loop oscillation modes in different operating conditions are shown in Table 2. It is clear that the damping ratio of the inter-area mode is low and the damping ratio of local mode 1 is not sufficient. To control inter-area

Table 1. Considered operating conditions.

Operating Condition	Characteristics
1	Transmitted power = 410 MW without any line outage
2	Transmitted power = 380 MW and outage one of lines between nodes 4 and 6
3	Transmitted power = 410 MW and outage one of lines between nodes 3 and 4

Table 2. Open-loop oscillation modes and their damping ratio.

Mode	Case 1	Case 2	Case 3
Local mod 1	$-1.243 \pm j7.744$ (15.85%)	$-1.146 \pm j7.769$ (14.59%)	$-1.242 \pm j7.744$ (15.84%)
Local mod 2	$-1.559 \pm j7.534$ (20.26%)	$-1.766 \pm j7.643$ (22.51%)	$-1.186 \pm j6.853$ (17.05%)
Inter-area mode	$-0.0469 \pm j1.838$ (2.551%)	$-0.080 \pm j1.561$ (5.19%)	$-0.013 \pm j1.794$ (0.725%)

Table 3. Residues for inter-area mode for different signals.

Operating Condition	SSSC-Based Damping Stabilizer	Input Signal		
		ΔI	ΔQ	ΔP
Case 1	ϕ-based	3.46∠ -153.23°	1.16∠-176.38°	3.23∠-151.76°
	m-based	0.64∠105.03°	0.28∠87.430°	0.65∠106.16°
Case 2	ϕ-based	2.40∠-130.95°	1.06∠-149.53°	2.33∠-130.20°
	m-based	0.552∠101.79°	0.243∠83.20°	0.538∠102.54°
Case 3	ϕ-based	3.21∠-148.79°	1.17∠-170.52°	3.07∠-149.84°
	m-based	0.59∠102.27°	0.21∠80.54°	0.56∠101.22°

oscillations, a SSSC is installed in the tie-line between nodes 5 and 6. Specific parameters used for the SSSC are given in the Appendix. Participation factors show that generators 1 and 2, especially generator 1, have the highest contribution to local mode 1. Generator 1 also has the highest contribution in the inter-area mode. A PSS to improve the damping ratio of the local mode is added to the exciter of generator 1. This PSS can significantly affect the inter-area mode. Therefore, coordination of PSS and SSSC-based stabilizers is necessary.

Table 3 shows residues for the inter-area mode under different operating conditions. This table shows that in some cases, the phase of residues is negative, therefore, the stabilizer must have a lag structure and, in other cases, it must have a lead structure. Also, this table confirms that the values of the residues for the SSSC-based stabilizer in the phase control channel are higher than those of the magnitude control channel.

In the following, the parameters of PSS and SSSC stabilizers are simultaneously calculated by the proposed method. It is assumed that the desired damping ratio for the inter-area and the local mode in each operating condition is $\zeta = 20\%$. According to the frequency of oscillation modes in the open-loop system, the value of $\bar{\omega}_q$ in Equation 31 has been considered $\bar{\omega}_q = 1, 5, 8$, and the time constants of the stabilizers for SSSC and PSS are set as $T = 0.4$ and 0.1, respectively. Also, the effects of stabilizers on other modes must be considered, so that the damping ratios of other modes have been increased, or do not become less than a specific value, and the variations of their frequencies must be acceptable.

To improve the damping ratios of the inter-area mode and local mode 1 to desired values, the parameters of the proposed SSSC-based stabilizers and PSS are calculated and shown in Tables 4 and 5. For comparison of SSSC-base stabilizers, the norm-1 is calculated according to the following equation:

$$\sum_{q=1}^{n_s} |f_q(j\omega))| . \tag{33}$$

Norm-1 at different values of ω is shown in Table 6. The results show that for the same desired damping ratio, norm-1 in the case of the SSSC ϕ-based stabilizer is less than in the case of the m-based stabilizer.

Table 4. Parameters of SSSC m-based stabilizer and PSS, 4-machine power system.

Operating Condition	Stabilizer	x_2	x_1	x_0
Case 1	SSSC	0.2064	0.1032	0.0129
	PSS	0.0152	0.1667	0.1516
Case 2	SSSC	0.0919	0.0459	0.0058
	PSS	0.0078	0.1457	0.6847
Case 3	SSSC	0.2318	0.1159	0.0145
	PSS	0.0152	0.1663	0.1512

Table 5. Parameters of SSSC ϕ-based stabilizer and PSS, 4-machine power system.

Operating Condition	Stabilizer	x_2	x_1	x_0
Case 1	SSSC	0.0021	0.0205	0.13700
	PSS	0.0067	0.0930	0.3100
Case 2	SSSC	0.0006	0.0095	0.0335
	PSS	0.0082	0.1464	0.6503
Case 3	SSSC	0.0019	0.0389	0.1372
	PSS	0.0089	0.1465	0.5756

Oscillation modes in the closed-loop system are shown in Tables 7 and 8. Comparing eigenvalues in open and closed- loop systems shows that damping ratios of the inter-area mode and the local mode have been improved to the desired values. In addition, it can be seen that other modes have not been degraded significantly.

For completeness and verification of the designed stabilizers, a three-phase fault is applied to the test system at bus 6 with fault duration of 0.02 s. The fault is cleared without line switching. Since generators 1 and 3 have the highest contribution to the inter-area mode, the swing angle of generator 1 with respect to generator 3 is shown in Figures 11 to 13. These figures

Table 6. The values of norm-1 at different values of ω, 4-machine power system.

Operating Condition	PSS and SSSC m-Based Stabilizer			PSS and SSSC ϕ-Based Stabilizer		
	ω (rad/s)			ω (rad/s)		
	2	**5**	**8**	**2**	**5**	**8**
Case 1	0.8435	1.726	2.1314	0.4081	0.4156	0.4740
Case 2	0.9156	1.1629	1.2435	0.6793	0.6957	0.7250
Case 3	0.9056	1.8518	2.2746	0.6829	0.6934	0.7424

Table 7. Closed-loop oscillation modes and their damping ratio in the case of PSS and SSSC m-based stabilizer.

Mode	Case 1	Case 2	Case 3
Local mod 1	$-1.575 \pm j7.341$ (20.98%)	$-1.549 \pm j7.779$ (19.52%)	$-1.572 \pm j7.342$ (20.94%)
Local mod 2	$-1.567 \pm j7.529$ (20.38%)	$-1.770 \pm j7.640$ (22.57%)	$-1.215 \pm j6.837$ (17.497%)
Inter-area mode	$-0.404 \pm j1.795$ (21.93%)	$-0.381 \pm j1.784$ (20.88%)	$-0.370 \pm j1.685$ (21.45%)

Table 8. Closed-loop oscillation modes and their damping ratio in the case of PSS and SSSC ϕ-based stabilizer.

Mode	Case 1	Case 2	Case 3
Local mod 1	$-1.578 \pm j7.628$ (20.25%)	$-1.597 \pm j7.730$ (20.23%)	$-1.632 \pm j7.670$ (20.81%)
Local mod 2	$-1.560 \pm j7.533$ (20.27%)	$-1.765 \pm j7.642$ (22.50%)	$-1.186 \pm j6.853$ (17.05%)
Inter-area mode	$-0.486 \pm j2.018$ (23.41%)	$-0.373 \pm j1.790$ (20.40%)	$-0.425 \pm j1.970$ (21.49%)

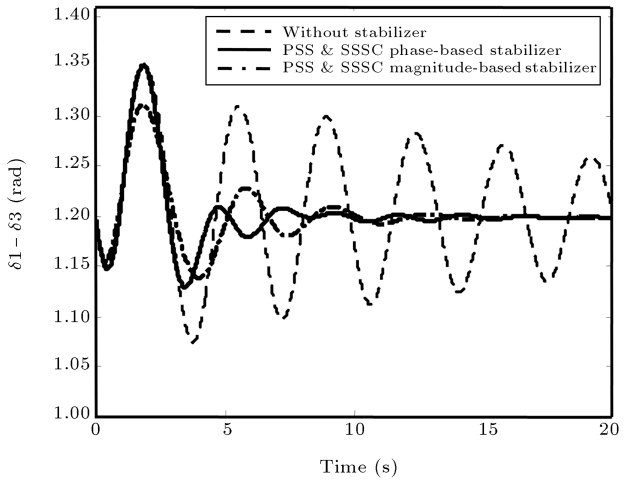

Figure 11. Swing angle of G1 relative to G3 for case 1.

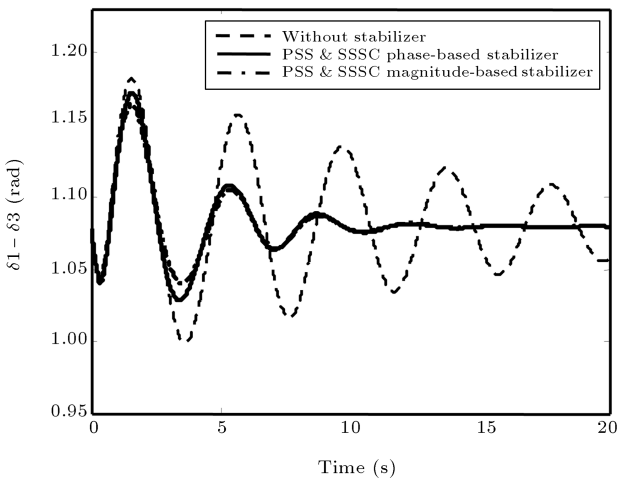

Figure 12. Swing angle of G1 relative to G3 for case 2.

show that SSSC-based stabilizers can effectively damp inter-area oscillations. Typically, in case 3, the control signals of SSSC stabilizers are shown in Figure 14. It can be seen that the ϕ-based stabilizer provides much less control effort compared to the m-based stabilizers.

Three-Area Six-Machine Power System

To confirm the obtained results on a 4-machine power system, in the following a 3-area 6-machine power system is investigated. A one-line diagram of the system is shown in Figure 15. Data of the system are represented in [22]. For increasing the transmitted power from area 1 to other areas, the real power of generators 3 and 4 and the load at bus 11 are increased. Inter-area modes and local modes in the open-loop system at light and heavy loading are listed in Table 9. Under light loading and heavy loading conditions, transmitted power is considered $P = 470$ MW and 750 MW, respectively. Mode shapes show that inter-area mode 1 consists of the machines of area 1 oscillating against the machines of areas 2 and 3, and inter-area mode 2 consists of the machines of area 2 oscillating against the machines of area 3. Because the damping ratio of inter-

Table 9. Inter-area and local modes and their damping ratio in open-loop system.

Mode	Light Loading	Heavy Loading
Inter-area mode 1	$-0.127 \pm j5.490$ (2.32%)	$-0.046 \pm j4.829$ (0.952%)
Inter-area mode 2	$-0.312 \pm j7.273$ (4.28%)	$-0.291 \pm j7.295$ (3.99%)
Local mode 1	$-1.373 \pm j12.358$ (11.04%)	$-1.348 \pm j12.378$ (10.83%)
Local mode 2	$-1.859 \pm j11.450$ (16.02%)	$-1.456 \pm j11.886$ (12.16%)
Local mode 3	$-2.392 \pm j11.256$ (20.79%)	$-2.328 \pm j11.289$ (20.19%)

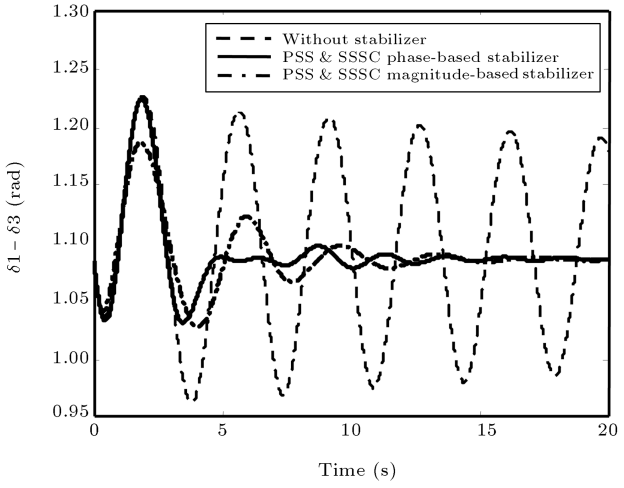

Figure 13. Swing angle of G1 relative to G3 for case 3.

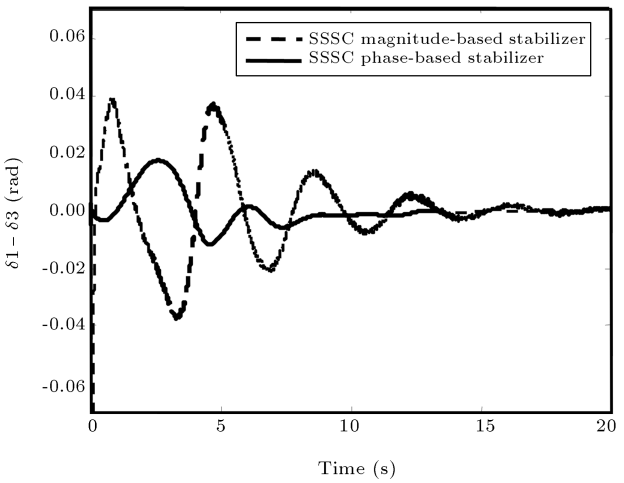

Figure 14. Control signals of SSSC stabilizers for case 3 with fault duration of 0.05s.

area mode 1 is low, a SSSC is installed on tie-line 8-11 to improve the damping ratio of this mode. Also, the damping ratio of local mode 1 related to the machines of area 3, and local mode 2 related to the machines of area 1, is not sufficient. Participation factors show that generator 2 and generator 4 are the best places for installing PSS to improve the damping of these local modes. Specific parameters used for SSSC are given in the Appendix.

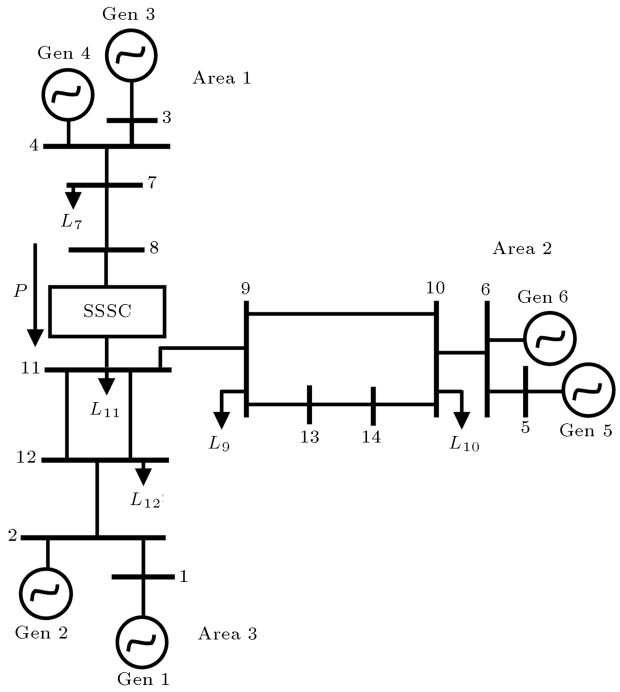

Figure 15. One-line diagram of 6-machine power system.

It is supposed that the minimum desired damping ratio for inter-area mode 1 is $\zeta = 15\%$ and for local modes is $\zeta = 20\%$. The time constant of the stabilizer for SSSC and PSS are set as $T = 0.2$ and 0.1s, respectively. Considering the variation of the line current as the input signal, the parameters of PSSs and SSSC stabilizers are shown in Tables 10 and 11. Closed-loop oscillation modes are shown in Tables 12 and 13.

Table 10. Parameters of PSS and SSSC ϕ-based stabilizer, 6-machine power system.

Operating Condition	Stabilizer	x_2	x_1	x_0
Light loading	SSSC	0.0167	0.2067	0.0092
	PSS2	0.0220	0.4078	1.8835
	PSS4	0.0073	0.1000	0.2658
Heavy loading	SSSC	0.0051	0.0135	0.0055
	PSS2	0.0265	0.4437	1.7823
	PSS4	0.0195	0.2686	0.7289

Table 11. Parameters of PSS and SSSC m-based stabilizer, 6-machine power system.

Operating Condition	Stabilizer	x_2	x_1	x_0
Light loading	SSSC	0.0164	0.0904	0.0411
	PSS2	0.0219	0.4379	2.1895
	PSS4	0.0184	0.2303	0.4901
Heavy loading	SSSC	0.0420	0.2255	0.1025
	PSS2	0.0222	0.4194	1.9757
	PSS4	0.0208	0.2876	0.8035

These tables show that in addition to the damping ratio of inter-area mode 1 the damping ratio of inter-area mode 2 is also significantly improved.

Norm-1 at different values of ω is shown in Table 14. Obtained results on a 6-machine power system like the obtained results on a 4-machine power system show that when the SSSC is installed on a tie-line that interconnects two areas in a multi-machine power system and a SSSC stabilizer is included in the phase control channel, it is more effective for damping inter-area oscillations.

Although in the 6-machine power system the results are shown for certain values of transmitted power, the same conclusion can be obtained for other values of transmitted power.

To show the performance of designed stabilizers under heavy loading conditions, a three-phase fault is applied to Bus 9 with fault duration of 0.02 s. The swing angle of generator 3, with respect to generator 6 for a SSSC stabilizer in different control channels, is shown in Figure 16. This figure shows that inter-area mode 1 is damped effectively.

CONCLUSION

In this paper, a method for the simultaneous coordinated tuning of a SSSC-based stabilizer and a PSS in a multi-machine power system is presented by quadratic mathematic programming. In this method,

Table 12. Inter-area and local modes and their damping ratio in closed-loop system in the case of PSS and SSSC m-based stabilizer.

Mode	Light Loading	Heavy Loading
Inter-area mode 1	$-0.920 \pm j6.012$ (15.12%)	$-0.781 \pm j5.035$ (15.32%)
Inter-area mode 2	$-0.986 \pm j7.382$ (13.24%)	$-0.943 \pm j7.397$ (12.64%)
Local mode 1	$-2.461 \pm j11.998$ (20.08%)	$-2.443 \pm j11.980$ (20.00%)
Local mode 2	$-2.374 \pm j11.339$ (20.49%)	$-2.409 \pm j11.462$ (20.57%)
Local mode 3	$-2.397 \pm j11.250$ (20.84%)	$-2.351 \pm j11.297$ (20.37%)

Table 13. Inter-area and local modes and their damping ratio in closed-loop system in the case of PSS and SSSC ϕ-based stabilizer.

Mode	Light Loading	Heavy Loading
Inter-area mode 1	$-0.991 \pm j6.288$ (15.56%)	$-0.793 \pm j5.047$ (15.52%)
Inter-area mode 2	$-1.307 \pm j7.569$ (17.01%)	$-0.958 \pm j7.280$ (13.04%)
Local mode 1	$-2.530 \pm j12.024$ (20.59%)	$-2.390 \pm j11.690$ (20.03%)
Local mode 2	$-2.409 \pm j11.302$ (20.85%)	$-2.359 \pm j11.501$ (20.09%)
Local mode 3	$-2.711 \pm j10.906$ (24.12%)	$-2.366 \pm j11.315$ (20.47%)

Table 14. The values of norm-1 at different values of ω, 6-machine power system.

Operating Condition	PSS and SSSC m-Based Stabilizer			PSS and SSSC ϕ-Based Stabilizer		
	ω (rad/s)			ω (rad/s)		
	5	8	12	5	8	12
Light loading	3.4027	3.7371	4.0059	2.5696	2.8172	3.0191
Heavy loading	3.9353	4.3986	4.7643	3.1497	3.6082	4.0184

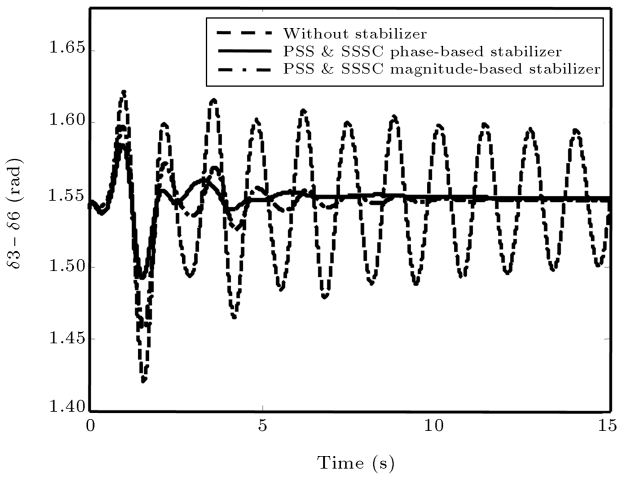

Figure 16. Swing angle of G3 relative to G6 for heavy loading.

the gain and phase of the stabilizer are calculated simultaneously. This method is not time-consuming and the parameters of stabilizers can be calculated by a few iterations. By this method, the influence of a SSSC-based stabilizer in different control channels on damping inter-area oscillations has been investigated. Analytical expression for the comparison of effects of SSSC-based stabilizers in different control channels on damping inter-area oscillation, if not impossible, is very difficult. However, obtained results under different operating conditions on a 2-area and 3-area power system interconnected with a weak tie line show that a SSSC-based stabilizer in the phase control channel (ϕ-based stabilizer) is more effective for damping inter-area oscillation than a magnitude-based stabilizer (m-based stabilizer). In the case of a ϕ-based stabilizer, to achieve the same desired value of damping ratio, control cost, i.e. the value of the stabilizer loop gain is lower than the m-based stabilizer. It seems that the results can be generalized to other multi-machine power systems interconnected with tie-lines, because an inter-area mode consists of machines in an area oscillating against the machines of that or other areas, as the studied systems.

REFERENCES

1. Kazemi, A. and Karimi, E. "The effect of an interline power flow controller (IPFC) on damping inter-area oscillations in interconnected power systems", *Scientia Iranica*, **15**(2), pp. 211-216 (2008).
2. Hessami Naghshbandi, A. et al. "An investigation on the performance of approximate methods in the representation of stressed power system", *Scientia Iranica, Trans. D, Comp. Science and Elec. Eng.*, **16**(1), pp. 74-83 (2009).
3. Noroozian, M. et al. "A robust control strategy for shunt and series reactive compensators to damp electromechanical oscillations", *IEEE Trans. Power Del.*, **16**(4), pp. 812-817 (2001).
4. Gyugyi, L. et al. "Static synchronous series compensator: a solid-state approach to the series compensation of transmission lines", *IEEE Trans. Power Del.*, **12**(1), pp. 406-417 (1997).
5. Haque, M.H. "Damping improvement by FACTS devices: A comparison between STATCOM and SSSSC", *J. of Elect. Power Syst. Res.*, **73**, pp. 177-185 (2005).
6. Chen, J. et al. "Enhancement of power system damping using VSC-based series connected FACTS controllers", *IEE Proc. - Gener. Transm. Distrib.*, **150**(2), pp. 353-359 (2003).
7. Farsangi, M.M. et al. "Choice of FACTS devices control inputs for damping inter-area oscillations", *IEEE Trans. PWRS*, **19**(2), pp. 1135-1142 (2005).
8. Castro, M.S. et al. "Impacts of FACTS controllers on damping power systems low frequency electromechanical oscillations", *IEEE-PES: Transm. Distrib. Conf. and Exp.* (2004).
9. Wang, H.F. "Static synchronous series compensator to damp power system oscillation", *J. of Elect. Power Syst. Res.*, **54**(8), pp. 113-119 (1999).
10. Kazemi, A. et al. "Optimal selection of SSSC Based damping stabilizer parameters for improving power system dynamic stability using genetic algorithm", *Iranian Journal of Science & Technology, Transaction B, Engineering*, **29**(B1), pp. 1-10 (2005).
11. Rigby, G.S. et al. "Analysis of a power oscillation damping scheme using a voltage-source inverter", *IEEE Trans. Indust. Appl.*, **38**(4), pp. 1105-1113 (2002).
12. Park, J.W. et al. "New external neuro-controller for series capacitive reactance compensator in a power network", *IEEE Trans. PWRS*, **19**(3), pp. 1462-1472 (2004).
13. Jowder, F.A.L. and Ooi, B.T. "Series compensation of radial power system by a combination of SSSC and dielectric capacitors", *IEEE Trans. PWRS*, **20**(1), pp. 458-465 (2005).
14. Pourbeik, P. and Gibbard, M.J. "Damping and synchronizing torques induced on generators by FACTS stabilizers in multi-machine power systems", *IEEE Trans. PWRS*, **11**(4), pp. 1920-1925 (1996).
15. Pourbeik, P. and Gibbard, M.J. "Simultaneous coordination of power system stabilizers and FACTS device stabilizers in a multi-machine power system for enhancing dynamic performance", *IEEE Trans. PWRS*, **13**(2), pp. 743-479 (1998).
16. Da Cruz, J.J. and Zanetta, J.J. "Stabilizer design for multi-machine power system using mathematical programming", *Int. J. Elec. Power Energy. Syst.*, **19**(8), pp. 519-523 (1997).
17. Zanetta, L.C. and Da Cruz, J.J. "An incremental approach to the coordinated tuning of power system stabilizers using mathematical programming", *IEEE Trans. PWRS*, **20**(1), pp. 895-902 (2005).

18. Sauer, P. and Pai, M., *Power System Dynamics and Stability*, Prentice Hall, New Jersey (1998).

19. Anderson, P.M. and Fouad, A.A., *Power System Control and Stability*, Iowa, Iowa State Univ. Press (1977).

20. Dorf, R.C. and Bishop, R.H., *Modern Control Systems*, Prentice Hall (2005).

21. Liu, S. et al. "Assessing placement of controllers and nonlinear behavior using normal form analysis", *IEEE Trans. PWRS*, **20**(3), pp. 1486-1495 (2005).

22. Taranto, G.N. et al. "Robust decentralized control design for damping power system oscillation", *The 33rd IEEE Conf. on Decision and Control*, Orlando, Florida, pp. 4080-4085 (1994).

APPENDIX

Specific parameters used for SSSC (all in p.u. except where indicated):

- 4-machine power system:

$$T_S = 0.01 \text{ s}, \qquad X_{\text{SCT}} = 0.15, \qquad C_{dc} = 1,$$

$$V_{dc\text{ref}} = 1, \qquad K_P = 25, \qquad K_I = 200.$$

- 6-machine power system:

$$T_S = 0.01 \text{ s}, \qquad X_{\text{SCT}} = 0.15, \qquad C_{dc} = 1,$$

$$V_{dc\text{ref}} = 1, \qquad K_P = 26, \qquad K_I = 100.$$

BIOGRAPHIES

Mahmoud Reza Shakarami was born in Khorramabad, Iran, in 1972. In 2000, he received his M.S. degree in Electrical Engineering from Iran University of Science and Technology in Tehran, Iran, where he is currently a Ph.D. candidate. His current research interests are: Power System Dynamics and Stability and FACTS Devices.

Ahad Kazemi was born in Tehran, Iran, in 1952. He received his M.S. degree in Electrical Engineering from Oklahoma State University, USA, in 1979 and is currently an Associated Professor in Electrical Engineering Department of Iran University of Science and Technology, in Tehran, Iran. His research interests are: Reactive Power Control, Power System Dynamics and FACTS Devices.